AIMS Mathematics, 9(7): 18083–18102.
DOI:10.3934/math.2024882
Received: 20 March 2024
Revised: 26 April 2024
Accepted: 29 April 2024
Published: 28 May 2024

https://www.aimspress.com/journal/Math

Research article

A kinetic non-steady state analysis of immobilized enzyme systems with external mass transfer resistance

M. Sivakumar[1], **M. Mallikarjuna**[2] **and R. Senthamarai**[2,*]

[1] Department of Mathematics, College of Science and Humanities, SRM Institute of Science and Technology, Vadapalani, Chennai 600026, Tamilnadu, India

[2] Department of Mathematics, College of Engineering and Technology, SRM Institute of Science and Technology, Kattankulathur 603203, Tamilnadu, India

* **Correspondence:** Email: senthamr@srmist.edu.in.

Abstract: The goal of this paper is to utilize the homotopy perturbation method (HPM) and Laplace transform to provide an approximate analytical expression to the non-linear time-dependent reaction diffusion equation arising in a mathematical model of an immobilized enzyme system with external mass transfer resistance. This mathematical model is a non-steady, non-linear reaction diffusion equation based on Michaelis–Menten kinetics. Approximate analytical expressions are also provided for various geometries of the enzyme catalytic pellets, namely, planar, cylindrical, and spherical. Obtained semi-analytical expressions are proven to fit for all the parameters appearing in the system and for all the geometries of enzyme catalytic pellets. When comparing the numerical and approximate analytical solutions, satisfactory results are obtained. Also, approximate analytical expressions of the effectiveness factor (EF) of the immobilized system are presented, and the effect of parameters on the EF is also analyzed.

Keywords: mathematical modelling; immobilized enzyme; Michaelis–Menten kinetics; homotopy perturbation method; Laplace transform technique
Mathematics Subject Classification: 35A22, 35A35, 35G31, 97M60

Nomenclature

Symbol	Meaning	Units [8]
X	Radial dimension inside the catalyst	m
T	Time	s
$c(X,T)$	Substrate concentration	$\mu mol/cm^3$
c_b	Bulk substrate concentration	$\mu mol/cm^3$
V_{max}	Maximum enzymatic rate	mol/s
D_e	Diffusion constant	m^2/s
R	Half the thickness of the pellets	m
K_m	Michaelis–Menten constant	$\mu mol/cm^3$
k_l	External mass transfer coefficient	m/s
x	Dimensionless radial dimension inside the catalyst	-
t	Dimensionless time	-
$C(x,t)$	Dimensionless substrate concentration	-
g	Shape factor of the pellet	-
α	Thiele modulus	-
β	Dimensionless Michaelis–Menten constant	-
B_i	Biot number	-

1. Introduction

The immobilization of enzymes on suitable materials has significantly increased their utilization in continuous bioreactors, biosensors, and batch reactors. However, these kinds of enzymes have several affecting factors that significantly differ from the kinetics of the non-immobilized enzyme. These factors encompass interparticle and intraparticle diffusion limitations, steric and conformational effects, and the partitioning of the substrate between the support and the bulk solution. The partitioning of the substrate between the support and the bulk solution, as well as conformational and spatial effects resulting from the immobilization mechanism, can lead to alterations in the enzyme's structure [1–3]. Measured reaction rates are influenced by the limitations in mass transfer that arise from the bulk phase to the support pellet's external surface [4]. The factors that influence the diffusion of the substrate in the bulk fluid phase include the diffusivity, velocity, density, viscosity, and substrate concentration of the fluid phase over the support pellets [5, 6]. Hamilton et al. [7] discussed in detail basic concepts in the effects of mass transfer on immobilized enzyme kinetics, which were illustrated by analyzing simple examples and determining the values of intrinsic kinetic parameters of immobilized enzymes.

Previously, various mathematical models considering the mass transfer resistance in the immobilized enzyme kinetics have been successfully applied in various fields using enzymatic kinetics. Mireshghi et al. [8] proposed a mathematical model for estimating the mass transfer of the enzymes immobilized onto the nonporous medium. Di Serio et al. [9] have developed a mathematical model describing the effect of limitation in oxygen mass transfer in the fed-batch reactor for growing baker's yeast. Gan et al. [10] analyzed experimentally and mathematically the influence of internal and external mass transfer resistance and interaction between the non-hyderolytic materials in the heterogeneous reaction system of cellulose hydrolysis. Al-Muftah and Abu-Reesh developed mathematical models

for estimating and simulating the performance of a packed-bed reactor for lactose hydrolysis, with the effect of internal [11] and external [12] mass transfer and inhibition of product concentrations. Baronas et al. [13] modeled a microbioreactor continuous mode of flowing of the substrate on a catalyzed enzyme and observed that the internal and external mass transfer had a non-linear effect on the system. A model explaining the process of mass transfer between lactitol and sucrose molecules during the osmotic dehydration of cherry was proposed by Maldonado and Peacheco [14].

Recently, Sivakumar et al. analyzed a mathematical model of immobilized enzyme kinetics, where the model is considered without the mass transfer effect, and obtained semi-analytical solutions for the concentration of substrate and EF at steady-state [15] conditions. The effect of existing parameters of the system on the EF of enzyme kinetics is also discussed. They also provided approximate analytical expressions for substrate concentration and EF for steady-state enzyme kinetics with the effect of external mass transfer resistance by using Taylor's series method [16].

Nevertheless, the aforementioned approach is restricted to the steady-state condition of enzymatic kinetics in an immobilized state. Recently, various iteration-based numerical and analytical techniques have been developed to solve the non-linear time-dependent partial differential equations. Shi and Yang [17] utilized the time-two-grid finite difference scheme for the first time to provide a numerical solution for the non-linear generalized viscous Burger's equation. Li et al. [18] proposed a new numerical scheme for solving the non-linear fourth-order Burgers' type equation with a weakly singular kernel known as the non-linear compact difference scheme. Shi and Yang [19] utilized the pointwise error estimate of a three-level conservative difference scheme for the supergeneralized viscous Burgers' equation. Atta and Hassan Youssri [20] provided a numerical solution for the third-order time-fractional Korteweg-De Vries Burgers' equation by utilizing the shifted second-kind Chebyshev polynomials and selecting the trail function as compatible with the governing equations. Yang et al. [21] formulated a higher-order method based on the orthogonal spine collocation method for solving the fourth-order subdiffusion problem on the rectangle domain in 2D with sides parallel to the coordinate axes. Zhou et al. [22] constructed an efficient numerical scheme evolution equation with three weakly singular kernels in three-dimensional space by making use of the backward Euler alternating direction implicit (ADI) method for the time derivative and the first-order convolution quadrature formula to deal with the Riemann–Liouville (R-L) fractional integral term. Researchers prefer obtaining approximate analytical expressions over numerical solutions due to difficulty in achieving numerical stability, adjusting parameters to match numerical data, and evaluating essential parameters.

The analytical method, namely the Laplace homotopy perturbation method (LHPM), has been recently used by researchers to obtain an approximate analytical solution for the non-linear partial differential equations arising in various fields of research. This method is a combination of two well-known analytical methods: the homotopy perturbation method and the Laplace transform method. By utilizing this method, a highly precise solution can be obtained in a very small number of iterations, which was first proposed by Madani et al. [23] in 2011. Yavuz and Sene [24] coupled this method with the heat balance integral method and successfully solved the fractional incompressible fluid differential equations. Recently, Sivakumar et al. [25] utilized the HPM with Laplace transform to provide an approximate analytical solution for the time-dependent non-linear partial differential equation arising in the enzymatic kinetics of the immobilized enzyme system without considering the mass transfer resistance. They have also provided semi-analytical expressions for all three geometries of the catalytic

pellets and the effectiveness factor of the system. As far as the authors are aware, no previous work has presented the approximate analytical expression for the non-steady, non-linear reaction diffusion equation of the immobilized enzyme, which is immobilized onto the nonporous medium with the effect of external mass transfer resistance.

In this paper, the main contributions are as follows:

- We have provided an approximate analytical expression for the time-dependent non-linear reaction diffusion equation of the substrate concentration and effectiveness factor of immobilized enzymes on the nonporous medium by utilizing the homotopy perturbation method and Laplace transform.
- The numerical simulation of the system is done using the MATLAB software, and the analytical expressions are compared with the numerical solution.
- Semi-analytical expressions for the substrate concentration and effectiveness factor of planar, cylindrical, and spherical geometries of the enzyme catalytic pellets are also provided using HPM and the Laplace transform. The sensitivity of EF to the parameters present in the system is also analyzed.

The work in this article is articulated as follows: in Section 2, we have presented the mathematical model of an immobilized enzyme system with external mass transfer resistance. In Section 3, the approximate analytical solution of the considered governing equation is provided by using the HPM and Laplace transform methods, and Section 4 provides the analytical expressions for various geometries of the catalytic pellets, namely, planar, cylindrical, and spherical. Section 5 demonstrates the validity of the obtained approximate analytical solutions by comparing them with the numerical simulation, presenting the graphical representation, and providing the error table. In Section 6, we illustrate the main result with graphical representations, and subsections 6.1 and 6.2 provide the effect of time and other parameters on the effectiveness factor of the system. Section 7 provides the research conclusion and future work. Finally, Section 7 provides the methodology to obtain the approximate analytical expression of the governing equation using HPM and the Laplace transform.

2. Mathematical model

A non-steady-state, non-linear enzyme kinetics model of immobilized enzymes is made by assuming:

1) Michaelis–Menten kinetics is utilized to describe the kinetics, which is represented as

$$v = \frac{V_{max}[S]}{K_m + [S]},$$

where v is the rate of reaction of the system, V_{max} is the maximum rate of reaction attained by the enzyme, K_m is the Michaelis–Menten constant, and S represents the substrate taking part in the reaction.

2) Support material is uniformly distributed by the enzyme.
3) Between the support and bulk fluid phases, the effect of partition is neglected.
4) With the support material, the effects of diffusivity and temperature are constant.
5) By considering the variation in time, a non-steady-state model is developed.

6) The deactivation of enzymes is neglected.

By making use of the above assumptions, the time-dependent partial differential equation with the boundary conditions expressing the concentration of substrate with mass transfer is obtained as follows:

$$\frac{\partial c(X,T)}{\partial T} = D_e\left(\frac{\partial c(X,T)}{\partial X^2} + \frac{g-1}{X}\frac{\partial c(X,T)}{\partial X}\right) - \frac{V_{max}c(X,T)}{K_m + c(X,T)}, \tag{2.1}$$

with the initial condition as,

$$\text{at } T = 0,\ c(X,0) = 0, \tag{2.2}$$

and boundary as

$$\text{at } X = 0,\ c_x(0,T) = 0, \tag{2.3}$$

$$\text{at } X = R,\ c_x(R,T) = \frac{Rk_l}{D_e}(1-c). \tag{2.4}$$

where D_e is the diffusion constant and R is the half-thickness of the pellets, c is the dimensional substrate concentration, c_b is the substrate in bulk phase, and k_l is the external mass transfer coefficient. The above equations are made dimensionless by the following dimensionless parameters:

$$x = \frac{X}{R},\ t = \frac{T}{R^2},\ C = \frac{c}{c_b},\ \alpha = R\sqrt{\frac{V_{max}}{K_m D_e}},\ \beta = \frac{c_b}{K_m}, B_i = \frac{Rk_l}{D_e}, \tag{2.5}$$

the dimensionless governing equations from Eqs (2.1)–(2.4) are obtained as follows:

$$\frac{\partial C(x,t)}{\partial t} = \frac{\partial^2 C(x,t)}{\partial x^2} + \frac{g-1}{x}\frac{\partial C(x,t)}{\partial x} - \frac{\alpha^2 C(x,t)}{1+\beta C(x,t)}, \tag{2.6}$$

the governing equation has boundary conditions such as,

$$\text{when } t = 0,\ C(x,t) = 0, \tag{2.7}$$

$$\text{when } x = 0,\ \frac{\partial C(x,t)}{\partial x} = 0, \tag{2.8}$$

$$\text{when } x = 1,\ \frac{\partial C(x,t)}{\partial x} = B_i(1 - C(x,t)). \tag{2.9}$$

where $C(x,t)$ is the concentration of substrate, x indicates the radial dimension inside the catalyst, g is the shape factor of the pellet, α symbolizes the Thiele modulus, β represents the dimensionless Michaelis–Menten constant, t depicts dimensionless time, and B_i is the Biot number.
The EF of the system is represented as

$$\eta = \frac{g(1+\beta)}{\alpha^2}\left(\frac{\partial C}{\partial x}\right)_{x=1}. \tag{2.10}$$

3. Approximate analytical expressions of non-steady-state governing equation by utilizing HPM and Laplace transform

Obtaining the solution for non-linear differential equations arising in various fields of physics, biosciences, chemical engineering, and biochemical engineering has been a challenge for researchers for decades. For solving these non-linear differential equations, researchers have recently utilized various iteration techniques. These iteration techniques are HPM [25–27], homotopy analysis method [28, 29], decomposition of homotopy analysis method [30], Taylors series method [15, 16, 31, 32], Adomian decomposition method [33–35], Akbari–Ganji method [36, 37], variational iteration method [38, 39], etc.

In this research, we have applied HPM with Laplace transform to obtain a semi-analytical expression (see Section 7) for the time-dependent non-linear governing equations Eq (2.6) with the boundary conditions Eqs (2.7)–(2.9), and the expression is obtained as:

$$C(x,t) = B_i(1-l)\left[\sqrt{\frac{g}{a}}\frac{\cosh\left(x\sqrt{\frac{a}{g}}\right)}{\sinh\left(\sqrt{\frac{a}{g}}\right)} - \frac{g}{a}e^{-at} - 2g\sum_{n=0}^{\infty}\frac{(-1)^n e^{-t(gn^2\pi^2+a)}}{(gn^2\pi^2+a)}\cos(n\pi x)\right], \tag{3.1}$$

where $a = \frac{\alpha^2}{1+\beta}$, and

$$l = \frac{D}{1+D}, \tag{3.2}$$

where

$$D = B_i\left[\sqrt{\frac{g}{a}}\coth\left(\sqrt{\frac{a}{g}}\right) - \frac{g}{a}e^{-at} - 2g\sum_{n=0}^{\infty}\frac{e^{-t(gn^2\pi^2+a)}}{(gn^2\pi^2+a)}\right], \tag{3.3}$$

and the EF of the system is represented as

$$\eta = \frac{g}{a}\,B_i\,(1-l). \tag{3.4}$$

4. Influence of geometries

4.1. Planar

When the shape factor value is $g = 1$, the shape of the catalytic pellet is planar, and the expression of concentration Eq (3.1) becomes

$$C(x,t) = B_i(1-l)\left[\sqrt{\frac{1}{a}}\frac{\cosh\left(\sqrt{a}x\right)}{\sinh\left(\sqrt{a}\right)} - \frac{e^{-at}}{a} - 2\sum_{n=0}^{\infty}\frac{(-1)^n e^{-t(n^2\pi^2+a)}}{(n^2\pi^2+a)}\cos(n\pi x)\right], \tag{4.1}$$

and by substituting the same for l in Eq (3.2), D transforms to

$$D = B_i\left[\sqrt{\frac{1}{a}}\coth\left(\sqrt{a}\right) - \frac{e^{-at}}{a} - 2\sum_{n=0}^{\infty}\frac{e^{-t(n^2\pi^2+a)}}{(n^2\pi^2+a)}\right], \tag{4.2}$$

and the EF of the planar pellet obtained by taking $g = 1$ in Eq (3.4)

$$\eta = \frac{1}{a}\left[B_i\,(1-l)\right]. \tag{4.3}$$

4.2. Cylindrical

When the shape factor value is $g = 2$, the shape of the catalytic pellet is cylindrical, and the expression of concentration Eq (3.1) becomes

$$C(x,t) = B_i(1-l)\left[\sqrt{\frac{2}{a}}\frac{\cosh\left(\sqrt{\frac{a}{2}}x\right)}{\sinh\left(\sqrt{\frac{a}{2}}\right)} - \frac{2}{a}e^{-at} - 4\sum_{n=0}^{\infty}\frac{(-1)^n e^{-t(2n^2\pi^2+a)}}{(2n^2\pi^2+a)}\cos(n\pi x)\right], \tag{4.4}$$

and by substituting the same for l in Eq (3.2), D transforms to

$$D = B_i\left[\sqrt{\frac{2}{a}}\coth\left(\sqrt{\frac{a}{2}}\right) - \frac{2}{a}e^{-at} - 4\sum_{n=0}^{\infty}\frac{e^{-t(2n^2\pi^2+a)}}{(2\,n^2\pi^2+a)}\right], \tag{4.5}$$

and the EF of a cylindrical pellet obtained by taking $g = 2$ in Eq (3.4)

$$\eta = \frac{2}{a}\left[B_i(1-l)\right]. \tag{4.6}$$

4.3. Spherical

When the shape factor value is $g = 3$, the shape of the catalytic pellet is spherical, and the expression of concentration Eq (3.1) becomes

$$C(x,t) = B_i(1-l)\left[\sqrt{\frac{3}{a}}\frac{\cosh\left(\sqrt{\frac{a}{3}}x\right)}{\sinh\left(\sqrt{\frac{a}{3}}\right)} - \frac{3}{a}e^{-at} - 6\sum_{n=0}^{\infty}\frac{(-1)^n e^{-t(3n^2\pi^2+a)}}{(3n^2\pi^2+a)}\cos(n\pi x)\right], \tag{4.7}$$

and by substituting the same for l in Eq (3.2), D transforms to

$$D = Bi\left[\sqrt{\frac{3}{a}}\coth\left(\sqrt{\frac{a}{3}}\right) - \frac{3}{a}e^{-at} - 6\sum_{n=0}^{\infty}\frac{e^{-t(3n^2\pi^2+a)}}{(3\,n^2\pi^2+a)}\right], \tag{4.8}$$

and the EF of the spherical pellet obtained by taking $g = 3$ in Eq (3.4)

$$\eta = \frac{3}{a}\left[B_i(1-l)\right]. \tag{4.9}$$

5. Validation of analytical result

The numerical solution of the non-linear time-dependent governing reaction-diffusion equation is obtained by using the MATLAB software. The approximate analytical expression for the time-dependent governing equation Eq (2.6) is obtained using HPM and the Laplace transform as Eq (3.1). The comparison of numerical and approximate analytical results for the non-steady state governing equations is shown in Figures 2–4 and Tables 1–3. The maximum error percentage obtained between numerical and HPM is 0.15%. Thus, HPM is more effective for obtaining the approximate analytical expression for the substrate concentration $C(x,t)$.

Table 1. Comparison of the approximate analytical result with numerical result of substrate concentration at planar geometry for the fixed $\alpha = 0.5$, $t = 10$, $B_i = 1$, and various values of β.

	$\beta = 1$			$\beta = 5$			$\beta = 10$		
χ	Numerical	HPM	Error%	Numerical	HPM	Error%	Numerical	HPM	Error%
0.0	0.31740	0.31734	0.01890	0.38320	0.38295	0.06524	0.41320	0.41290	0.07260
0.2	0.32624	0.32618	0.01839	0.39189	0.39164	0.06379	0.42165	0.42135	0.07115
0.4	0.35284	0.35278	0.01701	0.41781	0.41756	0.05984	0.44681	0.44651	0.06714
0.6	0.39746	0.39740	0.01510	0.46057	0.46032	0.05428	0.48811	0.48781	0.06146
0.8	0.46048	0.46042	0.01303	0.51947	0.51922	0.04813	0.54465	0.54435	0.05508
1.0	0.54239	0.54233	0.01106	0.59355	0.59330	0.04212	0.61514	0.61484	0.04877
Average error %			0.01558			0.05557			0.06270

Table 2. Comparison of the approximate analytical result with numerical result of substrate concentration at cylindrical geometry for the fixed $\alpha = 0.5$, $t = 10$, $B_i = 1$, and various values of β.

	$\beta = 1$			$\beta = 5$			$\beta = 10$		
χ	Numerical	HPM	Error%	Numerical	HPM	Error%	Numerical	HPM	Error%
0.0	0.56430	0.56410	0.03544	0.66820	0.66790	0.04490	0.70240	0.70160	0.11390
0.2	0.57022	0.57002	0.03507	0.67311	0.67281	0.04457	0.70691	0.70611	0.11317
0.4	0.58797	0.58777	0.03402	0.68769	0.68739	0.04362	0.72028	0.71948	0.11107
0.6	0.61742	0.61722	0.03239	0.71149	0.71119	0.04216	0.74200	0.74120	0.10782
0.8	0.65841	0.65821	0.03038	0.74381	0.74351	0.04033	0.77128	0.77048	0.10372
1.0	0.71072	0.71052	0.02814	0.78368	0.78338	0.03828	0.80705	0.80625	0.09913
Average error %			0.03257			0.04231			0.10813

Table 3. Comparison of the approximate analytical result with numerical result of substrate concentration at spherical geometry for the fixed $\alpha = 0.5$, $t = 10$, $B_i = 1$, and various values of β.

	$\beta = 1$			$\beta = 5$			$\beta = 10$		
χ	Numerical	HPM	Error%	Numerical	HPM	Error%	Numerical	HPM	Error%
0.0	0.71450	0.71417	0.04619	0.82210	0.82130	0.09731	0.85240	0.85110	0.15251
0.2	0.71841	0.71808	0.04593	0.82476	0.82396	0.09700	0.85468	0.85338	0.15210
0.4	0.73012	0.72979	0.04520	0.83264	0.83184	0.09608	0.86141	0.86011	0.15091
0.6	0.74951	0.74918	0.04403	0.84548	0.84468	0.09462	0.87232	0.87102	0.14903
0.8	0.77644	0.77611	0.04250	0.86286	0.86206	0.09271	0.88694	0.88564	0.14657
1.0	0.81071	0.81038	0.04071	0.88422	0.88342	0.09047	0.90467	0.90337	0.14370
Average error %			0.04409			0.09470			0.14914

6. Result and discussion

Equation (3.1) represents the novel semi-analytical expression of the non-steady non-linear governing equation Eq (2.6) with the boundaries Eqs (2.7)–(2.9) obtained by making use of HPM and Laplace transform. Equations (4.1), (4.4), and (4.7) represent the semi-analytical solution for planar, cylindrical, and spherical geometries of the catalytic pellets. Figure 1 represents the effect of dimensionless distance x and dimensionless time t on the substrate concentration $C(x,t)$ for planar 1(a), cylindrical 1(b), and spherical 1(c) shaped catalytic pellets. It is observed that the substrate concentration is an increasing function with respect to time and distance, and as their values increase, the concentration also increases.

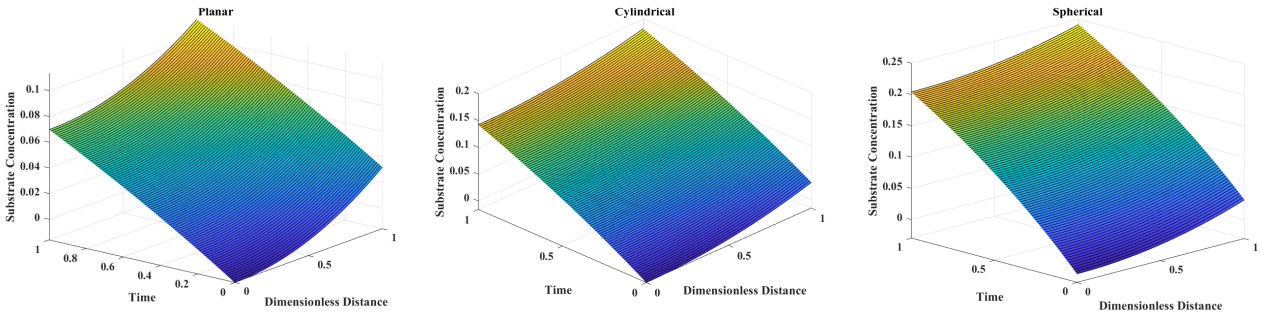

(a) **(b)** **(c)**

Figure 1. Surface plots of the concentration profile of substrate $C(x,t)$ with respect to the dimensionless distance and time for (a) planar, (b) cylindrical, and (c) spherical geometries.

Figures 2–4 depict the dimensionless concentration of substrate $C(x,t)$. From the figures, it is observed that the concentration is an increasing function with respect to the dimensionless distance x since the concentration is at its lowest value when $x = 0$ and reaches its maximum value when $x = 1$ for all the geometries of the enzyme. The impact of the parameters on the system is analyzed by varying the values of the dimensionless Michaelis–Menten constant β, the Thiele modulus α, and the Biot number B_i. From these figures, it is observed that β is directly proportional to the substrate since as the values of these parameters increase, the concentration also increases, which can be observed in Figures 2(a), 3(a) and 4(a), and the same can be observed for Biot number B_i which is observed in Figures 2(c), 3(c) and 4(c), whereas in the case of α, an increase in values decreases the concentration, which can be observed in Figures 2(b), 3(b) and 4(b).

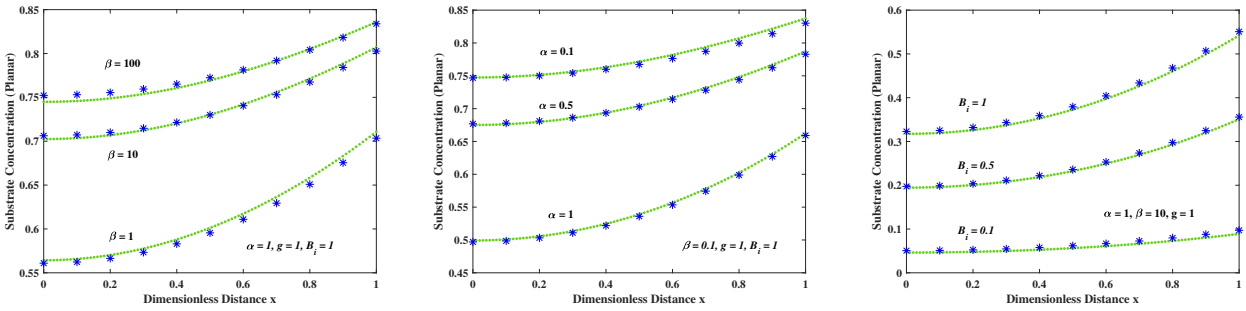

(a) **(b)** **(c)**

Figure 2. Comparison of dimensionless concentration profile of substrate versus the distance x of the planar pellets for (a) various values of β; (b) various values of α; (c) various values of B_i when $t = 5$, '$\cdots$' indicate the numerical results and '$***$' depict the analytical results by HPM.

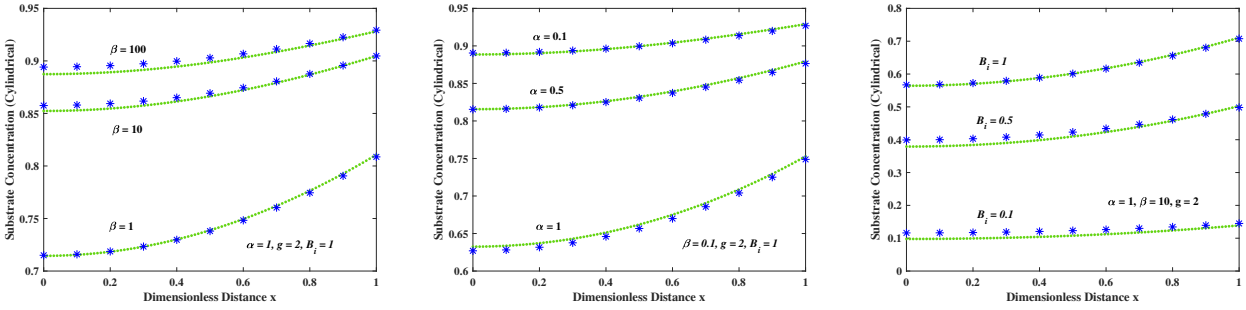

(a) **(b)** **(c)**

Figure 3. Comparison of dimensionless concentration profile of substrate versus the distance x of the cylindrical pellets for (a) various values of β; (b) various values of α; (c) various values of B_i when $t = 5$, '$\cdots$' indicate the numerical results and '$***$' depict the analytical results by HPM.

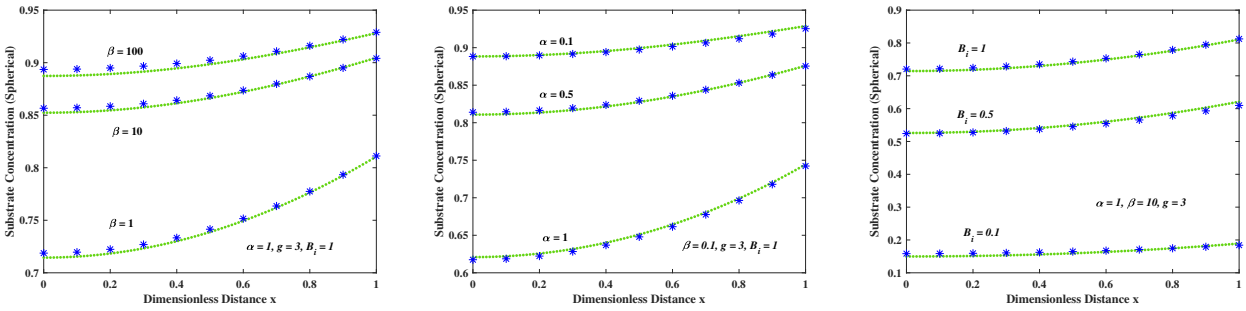

(a) **(b)** **(c)**

Figure 4. Comparison of dimensionless concentration profiles of substrate versus the distance x of the spherical pellets for (a) various values of β; (b) various values of α; (c) various values of B_i when $t = 5$, '$\cdots$' indicate the numerical results and '$***$' depict the analytical results by HPM.

6.1. Effectiveness factor

The effectiveness factor (EF) depicts the reaction rate ratio within the pellet to the reaction rate at its external surface. It is a unit-less metric ranging from 0 to 1, reflecting the efficiency of the catalyst. As the reaction rate increases throughout the entire volume of the pellet, η approaches 1, whereas η approaches its minimum when the pellet experiences a slower reaction. The semi-analytical expression for the EF of the system is presented in Eq (3.4). By substituting the values of $g = 1, 2, 3$, we get semi-analytical expressions for the EF of different geometric pellets, namely planar Eq (4.3), cylindrical Eq (4.6), and spherical Eq (4.9), which are derived using the HPM.

Figures 5–7 represent the variation in the effectiveness factor of the system with respect to the dimensionless time t in various geometries of catalytic pellets. It is seen that the effectiveness factor and the dimensionless time are directly proportional since, as the time increases, the effectiveness factor also increases for every geometric of catalytic pellets. It can be observed from the figures that the EF gradually increases with an increase in time, and then it attains equilibrium when $t \geq 10$. Also, when there is an increase in the dimensionless Michaelis–Menten constant β, the effectiveness factor also increases, as can be seen in Figures 5(a), 6(a), and 7(a), whereas in the case of the Thiele modulus α, as it increases, the effectiveness factor decreases gradually, as can be observed in Figures 5(b), 6(b), and 7(b).

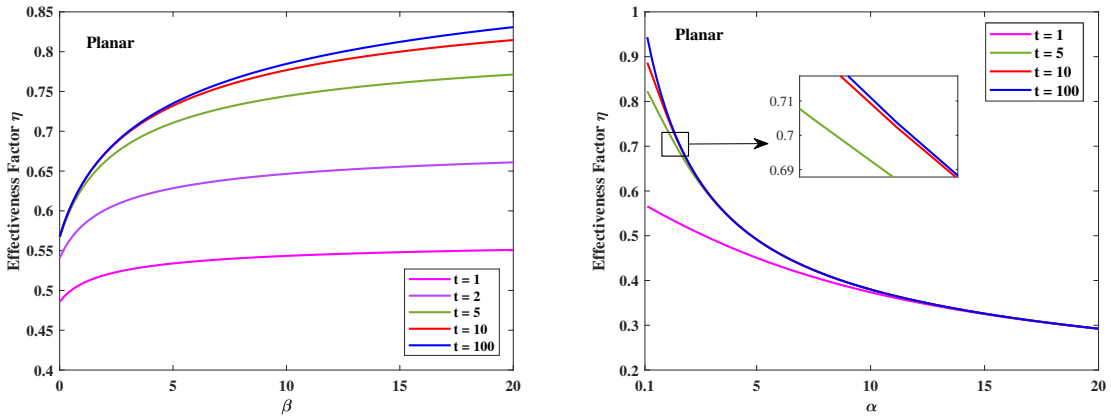

Figure 5. Effectiveness factor versus (a) Michaelis–Menten constant β for fixed parameters $\alpha = 1$ and $B_i = 1$; (b) Thiele modulus α for fixed parameters $\beta = 10$ and $B_i = 1$ for various values of time t for planar pellets.

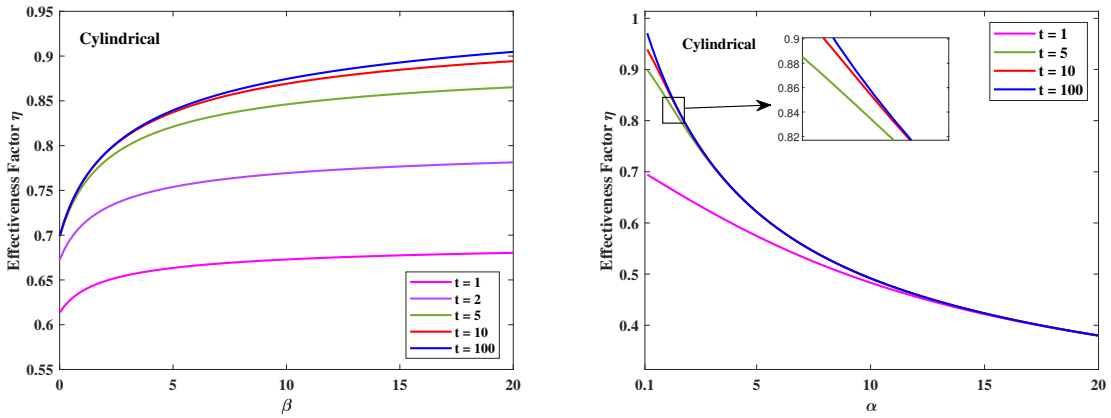

Figure 6. Effectiveness factor versus (a) Michaelis–Menten constant β for fixed parameters $\alpha = 1$ and $B_i = 1$; (b) Thiele modulus α for fixed parameters $\beta = 10$ and $B_i = 1$ for various values of time t for cylindrical pellets.

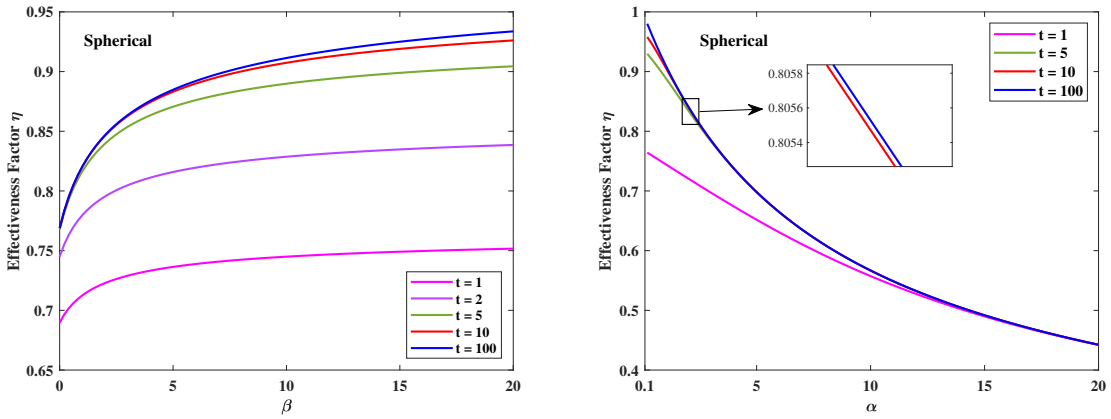

Figure 7. Effectiveness factor versus (a) Michaelis–Menten constant β for fixed parameters $\alpha = 1$ and $B_i = 1$; (b) Thiele modulus α for fixed parameters $\beta = 10$ and $B_i = 1$ for various values of time t for spherical pellets.

6.2. *Analysis of parameters sensitivity*

Partial derivatives with respect to the parameters indicate the degree of the solution's responsiveness to parameter changes. This study showcases the impact of each parameter on the system's EF in enzyme kinetics, identifying critical factors that significantly influence the system. Consequently, this analysis not only guides experimental design and optimization efforts but also enhances understanding of the system's robustness, reliability, and performance under varying conditions. Figure 8 depicts the influence and parameter effects on the EF of the system. Parametric values utilized for analysis are $\beta = 10$, $\alpha = 1$, $B_i = 1$, and $t = 5$.

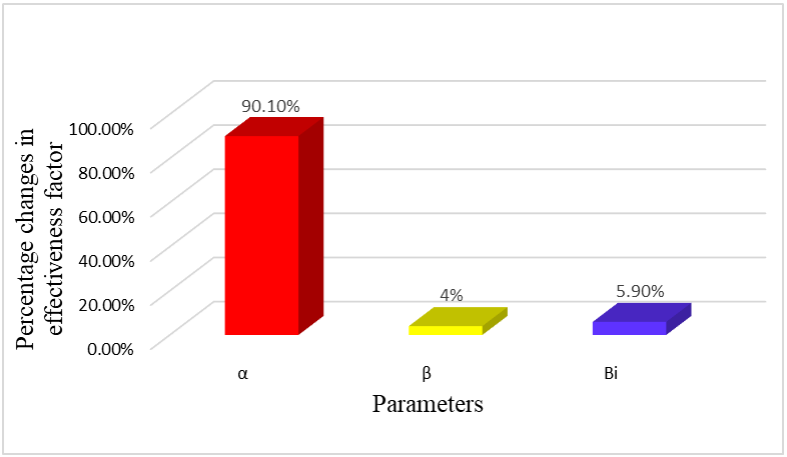

Figure 8. Parameters effect on effectiveness factor.

From Figure 8, it is observed that the Thiele modulus α has the most effect on the effective performance of the reaction diffusion of the system at 90%. This shows that the diffusion parameter D_e, the Michaelis–Menten constant K_m, and the maximum enzymatic rate V_{max} have a major effect on

the system. The second most affecting parameter is the biot number B_i, with 6%, which implies that the external mass transfer resistance affects the system considerably. The parameter that has the least effect on the EF is α at 4%, which shows that the bulk substrate concentration has less effect on the EF of the system.

7. Conclusions

The HPM and Laplace transform have been successfully applied to obtain an approximate analytical solution of the non-linear time-dependent reaction diffusion equation of the immobilized enzyme kinetic model with external mass transfer resistance and the effectiveness factor. Closed-form semi-analytical expressions of substrate concentration for planar, cylindrical, and spherical enzyme catalytic pellets and their corresponding semi-analytical expressions of EF are also derived and analyzed. The obtained semi-analytical expression is compared with the numerical solution using the MATLAB program to achieve satisfactory results for all parameter values. It is found that the effectiveness factor of the system is most sensitive to the Thiele modulus α, followed by Biot number B_i.

The obtained analytical expressions provide a precise understanding of the enzyme kinetics of the immobilized enzyme system with mass transfer resistance, which can be utilized in the areas where immobilized enzymes are used, namely, biosensors, batch reactors, food, textile, and pharmaceutical industries. This proposed method can be applied to solve time-dependent partial differential problems that arise in various fields of research.

Author Contributions

M. Sivakumar: data curation, methodology, visualization, formal analysis, writing-original draft; M. Mallikarjuna: visualization, methodology, investigation, software, writing-original draft; R. Senthamarai: conceptualization, methodology, resources, investigation, validation, supervision, writing-review and editing. All authors have read and approved the final version of the manuscript for publication.

Use of AI tools declaration

The authors declare that they have not used Artificial Intelligence (AI) tools in the creation of this article.

Acknowledgment

The authors are very much thankful to the management, SRM Institute of Science and Technology for their continuous support and encouragement.

Conflict of interest

The authors declare that they have no conflict of interest.

References

1. P. J. Halling, R. V. Ulijn, S. L. Flitsch, Understanding enzyme action on immobilised substrates, *Curr. Opin. Biotech.*, **16** (2005), 385–392. https://doi.org/10.1016/j.copbio.2005.06.006
2. T. Kobayashi, K. J. Laidler, Theory of the kinetics of reactions catalyzed by enzymes attached to membranes, *Biotechnol. Bioeng.*, **16** (1974), 77–97. https://doi.org/10.1002/bit.260160107
3. A. Kheirolomoom, K. Shigeo, E. Sada, K. I. Yoshida, Reaction characteristics and stability of a membrane-bound enzyme reconstituted in bilayers of liposomes, *Biotechnol. Bioeng.*, **37** (1991), 809–813. https://doi.org/10.1002/bit.260370904
4. S. Gondo, S. Isayama, K. Kusunoki, Effects of internal diffusion on the lineweaver-Burk plots for immobilized enzymes, *Biotechnol. Bioeng.*, **17** (1975), 423–431. https://doi.org/10.1002/bit.260170310
5. A. Illanes, M. E. Zuniga, S. Contreras, A. Guerrero, Reactor design for the enzymatic isomerization of glucose to fructose, *Bioprocess Engineering*, **7** (1992), 199–204. https://doi.org/10.1007/BF00369546
6. C. Picioreanu, M. C. M. van Loosdrecht, J. J. Heijnen, Effect of diffusive and convective substrate transport on biofilm structure formation: A two-dimensional modeling study, *Biotechnol. Bioeng.*, **69** (2000), 504–515. https://doi.org/10.1002/1097-0290(20000905)69:5%3C504::AID-BIT5%3E3.0.CO;2-S
7. B. K. Hamilton, C. R. Gardner, C. K. Colton, Basic concepts in the effects of mass transfer on immobilized enzyme kinetics, In: *Immobilized enzymes in food and microbial processes*, Boston: Springer, 1974, 205–224. https://doi.org/10.1007/978-1-4684-2088-3_12
8. S. A. Mireshghi, A. A. Kheyr, F. Khorasheh, Application of an optimization algorithm for estimation of substrate mass transfro parameters for immobilized enzyme reactions, *Sci. Iran.*, **8** (2001), 189–196.
9. M. Di Serio, R. Tesser, E. Santacesaria, A kinetic and mass transfer model to simulate the growth of baker's yeast in industrial bioreactors, *Chem. Eng. J.*, **82** (2001), 347–354. https://doi.org/10.1016/S1385-8947(00)00353-3
10. Q. Gan, S. J. Allen, G. Taylor, Kinetic dynamics in heterogeneous enzymatic hydrolysis of cellulose: an overview, an experimental study and mathematical modelling, *Process Biochem.*, **38** (2003), 1003–1018. https://doi.org/10.1016/S0032-9592(02)00220-0
11. A. E. Al-Muftah, I. M. Abu-Reesh, Effects of internal mass transfer and product inhibition on a simulated immobilized enzyme-catalyzed reactor for lactose hydrolysis, *Biochem. Eng. J.*, **23** (2005), 139–153. https://doi.org/10.1016/j.bej.2004.10.010
12. A. E. AL-Muftah, I. M. Abu-Reesh, Effects of external mass transfer and product inhibition on a simulated immobilized enzyme-catalyzed reactor for lactose hydrolysis, *Eng. Life Sci.*, **4** (2004), 326–340. https://doi.org/10.1002/elsc.200401980
13. R. Baronas, J. Kulys, L. Petkevičius, Modelling the enzyme catalysed substrate conversion in a microbioreactor acting in continuous flow mode, *Nonlinear Anal. Model.*, **23** (2018), 437–456. https://doi.org/10.15388/NA.2018.3.9

14. M. Maldonado, J. G. Pacheco, Mathematical modelling of mass transfer phenomena for sucrose and lactitol molecules during osmotic dehydration of cherries, *Heliyon*, **8** (2022), e08788 https://doi.org/10.1016/j.heliyon.2022.e08788

15. M. Sivakumar, R. Senthamarai, L. Rajendran, M. E. G. Lyons, Reaction and kinetic studies of immobilized enzyme systems: part-I without external mass transfer resistance, *Int. J. Electrochem. Sc.*, **17** (2022), 221159. https://doi.org/10.20964/2022.09.69

16. M. Sivakumar, R. Senthamarai, L. Rajendran, M. E. G. Lyons, Reaction and kinetics studies of immobilized enzyme systems: part-II with external mass transfer resistance, *Int. J. Electrochem. Sc.*, **17** (2022), 221031. https://doi.org/10.20964/2022.10.43

17. Y. Shi, X. H. Yang, A time two-grid difference method for nonlinear generalized viscous Burger' equation, *J. Math. Chem.*, **2024** (2024), 1–34. https://doi.org/10.1007/s10910-024-01592-x

18. C. J. Li, H. X. Zhang, X. H. Yang, A new nonlinear compact difference scheme for a fourth-order nonlinear Burgers type equation with a weakly singular kernel, *J. Appl. Math. Comput.*, **2024** (2024), 1–33. https://doi.org/10.1007/s12190-024-02039-x

19. Y. Shi, X. H. Yang, Pointwise error estimate of conservative difference scheme for supergeneralized viscous Burgers' equation, *Electron. Res. Arch.*, **32** (2024), 1471–1497. http://doi.org/10.3934/era.2024068

20. A. G. Atta, Y. H. Youssri, Shifted second-kind Chebyshev spectral collocation-based technique for time-fractional KdV-Burgers' equation, *Iran. J. Math. Chem.*, **14** (2023), 207–224. http://doi.org/10.22052/IJMC.2023.252824.1710

21. X. H. Yang, H. X. Zhang, J. Tang, The OSC solver for the fourth-order sub-diffusion equation with weakly singular solutions, *Comput. Math. Appl.*, **82** (2021), 1–12. https://doi.org/10.1016/j.camwa.2020.11.015

22. Z. Y. Zhou, H. X. Zhang, X. H. Yang, J. Tang, An efficient ADI difference scheme for the nonlocal evolution equation with multi-term weakly singular kernels in three dimensions, *Int. J. Comput. Math.,* **100** (2023), 1719–1736. https://doi.org/10.1080/00207160.2023.2212307

23. M. Madani, M. Fathizadeh, Y. Khan, A. Yildirim, On the coupling of the homotopy perturbation method and Laplace transformation, *Math. Comput. Model.*, **53** (2011), 1937–1945. https://doi.org/10.1016/j.mcm.2011.01.023

24. M. Yavuz, N. Sene, Approximate solutions of the model describing fluid flow using generalized ρ-Laplace transform method and heat balance integral method, *Axioms*, **9** (2020), 123. https://doi.org/10.3390/axioms9040123

25. M. Sivakumar, M. Mallikarjuna, R. Senthamarai, A kinetic non-steady-state analysis of immobilized enzyme systems without external mass transfer resistance, *Int. J. Anal. Appl.*, **22** (2024), 31. https://doi.org/10.28924/2291-8639-22-2024-31

26. J. H. He, Homotopy perturbation method: a new nonlinear analytical technique, *Appl. Math. Comput.*, **135** (2003), 73–79. https://doi.org/10.1016/S0096-3003(01)00312-5

27. R. Senthamarai, R. J. Ranjani, Solution of non-steady-state substrate concentration in the action of biosensor response at mixed enzyme kinetics, *J. Phys.: Conf. Ser.*, **1000** (2018), 012138. https://doi.org/10.1088/1742-6596/1000/1/012138

28. A. Kumar, A. Khan, R. Arora, T. Abdeljawad, K. Karthikeyan, M. Houas, Analysis of the far-field behavior of waves in magnetogasdynamic, *AIMS Mathematics*, **8** (2023), 7329–7345. https://doi.org/10.3934/math.2023369

29. Y. Yang, S. Liao, Comparison between homotopy analysis method and homotopy renormalization method in fluid mechanics, *Eur. J. Mech. B-Fluid.*, **97** (2023), 187–198. https://doi.org/10.1016/j.euromechflu.2022.10.005

30. O. Nave, Modification of semi-analytical method applied system of ODE, *Modern Applied Science*, **14** (2020), 75. https://doi.org/10.5539/mas.v14n6p75

31. Y. Ji, J. Liu, H. B. Liu, An identification algorithm of generalized time-varying systems based on the Taylor series expansion and applied to a pH process, *J. Process Contr.*, **128** (2023), 103007. https://doi.org/10.1016/j.jprocont.2023.103007

32. C. H. He, Y. U. E. Shen, F. Y. Ji, J. H. He, Taylor series solution for fractal Bratu-type equation arising in electrospinning process, *Fractals*, **28** (2020), 2050011. https://doi.org/10.1142/S0218348X20500115

33. A. M. Wazwaz, A reliable modification of Adomian decomposition method, *Appl. Math. Comput.*, **102** (1999), 77–86. https://doi.org/10.1016/S0096-3003(98)10024-3

34. M. Mallikarjuna, R. Senthamarai, An amperometric biosensor and its steady state current in the case of substrate and product inhibition: Taylors series method and Adomian decomposition method, *J. Electroanal. Chem.*, **946** (2023), 117699. https://doi.org/10.1016/j.jelechem.2023.117699

35. Y. Jawarneh, H. Yasmin, A. H. Ganie, M. M. Al-Sawalha, A. Ali, Unification of Adomian decomposition method and ZZ transformation for exploring the dynamics of fractional Kersten-Krasil'shchik coupled KdV-mKdV systems, *AIMS Mathematics*, **9** (2024), 371–390. https://doi.org/10.3934/math.2024021

36. S. Hosseinzadeh, K. Hosseinzadeh, M. Rahai, D. D. Ganji, Analytical solution of nonlinear differential equations two oscillators mechanism using Akbari-Ganji method, *Mod. Phys. Lett. B*, **35** (2021), 2150462. https://doi.org/10.1142/S0217984921504625

37. S. Saravanakumar, A. Eswari, O. D. Makinde, N. Anbazhagan, G. P. Joshi, W. Cho, Analysis of temperature-dependent thermal conductivity and fin efficiency: direct Akbari-Ganji method, *Case Stud. Therm. Eng.*, **51** (2023), 103627. https://doi.org/10.1016/j.csite.2023.103627

38. M. Adel, M. M. Khader, H. Ahmad, T. A. Assiri, Approximate analytical solutions for the blood ethanol concentration system and predator-prey equations by using variational iteration method, *AIMS Mathematics*, **8** (2023), 19083–19096. https://doi.org/10.3934/math.2023974

39. R. Senthamarai, T. N. Saibavani, Substrate mass transfer: analytical approach for immobilized enzyme reactions, *J. Phys.: Conf. Ser.*, **1000** (2018), 012146. https://doi.org/10.1088/1742-6596/1000/1/012146

Appendix

Approximate analytical solution of Eq (2.6) using HPM and Laplace transform

The homotopy for the governing equation is constructed as

$$(1-p)\left[\frac{\partial C}{\partial t}-\frac{\partial^2 C}{\partial x^2}-\frac{g-1}{x}\frac{\partial C}{\partial x}+\frac{\alpha^2 C}{1+\beta C(1,t)}\right]+p\left[\frac{\partial C}{\partial t}-\frac{\partial^2 C}{\partial x^2}-\frac{g-1}{x}\frac{\partial C}{\partial x}+\frac{\alpha^2 C}{1+\beta C}\right]=0, \quad (7.1)$$

we consider that when $t \to \infty$ the substrate concentration $C(1,t) \approx 1$ to linearize the equation for effective computation of the governing equation by utilizing HPM

$$(1-p)\left[\frac{\partial C}{\partial t}-\frac{\partial^2 C}{\partial x^2}-\frac{g-1}{x}\frac{\partial C}{\partial x}+\frac{\alpha^2 C}{1+\beta}\right]+p\left[\frac{\partial C}{\partial t}-\frac{\partial^2 C}{\partial x^2}-\frac{g-1}{x}\frac{\partial C}{\partial x}+\frac{\alpha^2 C}{1+\beta C}\right]=0, \quad (7.2)$$

the solution of the substrate concentration is given as

$$C(x,t) = C_0(x,t) + p\, C_1(x,t) + p^2\, C_2(x,t) + \cdots, \quad (7.3)$$

by substituting the above equation in Eq (7.2) and for the initial power of the p, we get

$$p^0: \quad \frac{\partial C_0}{\partial t}-\frac{\partial^2 C_0}{\partial x^2}-\frac{g-1}{x}\frac{\partial C_0}{\partial x}+aC_0=0, \quad (7.4)$$

where the constant $a = \frac{\alpha^2}{1+\beta}$.

Then, by applying the transform by Laplace method, we get

$$\frac{d^2\tilde{C}_0(x,s)}{dx^2}+\frac{g-1}{x}\frac{d\tilde{C}_0(x,s)}{dx}-(s+a)\,\tilde{C}_0(x,s)=0, \quad (7.5)$$

with the boundaries

$$\text{at} \quad x=0, \qquad \frac{d\tilde{C}_0(x,s)}{dx}=0, \quad (7.6)$$

$$\text{at} \quad x=1, \qquad \frac{d\tilde{C}_0(x,s)}{dx}=\frac{B_i(1-l)}{s}, \quad (7.7)$$

where $\tilde{C}_0(x,s)$is the Laplace transform of $C_0(x,t)$.
By utilizing the AGM the solution is assumed as

$$\tilde{C}_0(x,s) = A\cosh(mx) + B\sinh(mx), \quad (7.8)$$

by utilizing the boundary conditions Eqs (7.6) and (7.7) we obtain the solution of the substrate as

$$\tilde{C}_0(x,s) = \frac{B_i(1-l)\cosh(mx)}{ms\sinh(m)}, \quad (7.9)$$

by using the Eq (7.9) into Eq (7.5) the constant m is obtained as

$$m = \sqrt{\frac{s+a}{g}}. \quad (7.10)$$

By substituting the above values in Eq (7.9)

$$\tilde{C}_0(x,s) = \frac{B_i(1-l)\cosh\left(\sqrt{\frac{s+a}{g}}x\right)}{s\sqrt{\frac{s+a}{g}}\sinh\left(\sqrt{\frac{s+a}{g}}\right)}. \tag{7.11}$$

By using complex inversion formula

$$C_0(x,t) = \frac{1}{2\pi i}\int_{x-i\infty}^{x+i\infty} e^{st}\tilde{C}_0(x,s)ds = \text{sum of residues at all poles lie inside the range } (\mathrm{x} - \mathrm{i}\infty, \mathrm{x} + \mathrm{i}\infty). \tag{7.12}$$

Hence, in order to invert Eq (7.11) the residues are at $s = 0$, $s = -a$ are simple poles and the $s_n = -gn^2\pi^2 - a$, where $n = 1, 2, 3, \cdots$ generates infinitely many poles as the solution of $\sinh\left(\sqrt{\frac{s+a}{g}}\right) = 0$

$$\begin{aligned}\text{Res}\left[\frac{B_i\ (1-l)\ \cosh\left(x\sqrt{\frac{s+a}{g}}\right)}{s\ \sqrt{\frac{s+a}{g}}\ \sinh\left(\sqrt{\frac{s+a}{g}}\right)}\right] \;=\; &\text{Res}\left[\frac{Bi\ (1-l)\ \cosh\left(x\sqrt{\frac{s+a}{g}}\right)}{s\ \sqrt{\frac{s+a}{g}}\ \sinh\left(\sqrt{\frac{s+a}{g}}\right)}\right]_{s=0} \\ &+ \text{Res}\left[\frac{B_i\ (1-l)\ \cosh\left(x\sqrt{\frac{s+a}{g}}\right)}{s\ \sqrt{\frac{s+a}{g}}\ \sinh\left(\sqrt{\frac{s+a}{g}}\right)}\right]_{s=s_{-a}} \\ &+ \text{Res}\left[\frac{B_i\ (1-l)\ \cosh\left(x\sqrt{\frac{s+a}{g}}\right)}{s\ \sqrt{\frac{s+a}{g}}\ \sinh\left(\sqrt{\frac{s+a}{g}}\right)}\right]_{s=s_n}\end{aligned}, \tag{7.13}$$

the residue at $s = 0$ is given by

$$\text{Res}\left[\frac{Bi\ (1-l)\ \cosh\ \left(x\sqrt{\frac{s+a}{g}}\right)}{s\ \sqrt{\frac{s+a}{g}}\ \sinh\ \left(\sqrt{\frac{s+a}{g}}\right)}\right]_{s=0} = \lim_{s\to 0}\left[\frac{(s-0)e^{st}B_i(1-l)\cosh(\sqrt{\frac{s+a}{g}}x)}{\sqrt{\frac{s+a}{g}}\sinh(\sqrt{\frac{s+a}{g}})}\right]$$

$$= \frac{B_i\ (1-l)\ \cosh\ \left(x\sqrt{\frac{a}{g}}\right)}{\sqrt{\frac{a}{g}}\ \sinh\ \left(\sqrt{\frac{a}{g}}\right)}, \tag{7.14}$$

at $s = -a$

$$\text{Res}\left[\frac{B_i\ (1-l)\ \cosh\ \left(x\sqrt{\frac{s+a}{g}}\right)}{s\ \sqrt{\frac{s+a}{g}}\ \sinh\ \left(\sqrt{\frac{s+a}{g}}\right)}\right]_{s=-a} = \lim_{s\to -a}\left[\frac{(s+a)e^{st}\cosh(\sqrt{\frac{s+a}{g}}x)}{\sqrt{\frac{s+a}{g}}\sinh(\sqrt{\frac{s+a}{g}})}\right]$$

$$= -\frac{g\,B_i\ (1-l)}{a}\ e^{-at}, \tag{7.15}$$

and at $s = s_n$

$$\text{Res}\left[\frac{B_i\ (1-l)\ \cosh\ \left(x\sqrt{\frac{s+a}{g}}\right)}{s\ \sqrt{\frac{s+a}{g}}\ \sinh\left(\sqrt{\frac{s+a}{g}}\right)}\right]_{s=s_n} = \lim_{s\to s_n}\left[\frac{e^{st}\cosh(\sqrt{\frac{s+a}{g}}x)}{\frac{d}{ds}\sinh(\sqrt{\frac{s+a}{g}})}\right]$$

$$= -2g\,B_i\,(1-l)\sum_{n=0}^{\infty}\frac{e^{-t(gn^2\pi^2+a)}\cos(n\pi x)}{(gn^2\pi^2+a)}, \tag{7.16}$$

by adding Eqs (7.14)–(7.16) we get the solution expression, which is represented in Eq (3.1).
By substituting $x = 1$ in Eq (3.1) and upon simplification, we obtain the value of unknown l as in Eq (3.2).

AIMS Press